Design and Evaluation of a Smooth-Locking-Based Customizable Prosthetic Knee Joint

Kunyang Wang
Key Laboratory of Bionic Engineering, Ministry of Education,
Jilin University,
Changchun 130025, China
e-mail: kywang@jlu.edu.cn
ASME Member

Harry Williams
School of Mechanical, Aerospace and Civil Engineering,
The University of Manchester,
Manchester M13 9PL, UK
e-mail: harry_williams@yeah.net

Zhihui Qian
Key Laboratory of Bionic Engineering, Ministry of Education,
Jilin University,
Changchun 130025, China
e-mail: zhqian@jlu.edu.cn

Guowu Wei
School of Science, Engineering and Environment,
University of Salford,
Salford M5 4WT, UK.
e-mail: g.wei@salford.ac.uk
ASME Member

Haohua Xiu
Key Laboratory of Bionic Engineering, Ministry of Education,
Jilin University,
Changchun 130025, China
e-mail: xiuhh@jlu.edu.cn

Wei Chen
Key Laboratory of Bionic Engineering, Ministry of Education,
Jilin University,
Changchun 130025, China
e-mail: chenwei_jlu@jlu.edu.cn

Xuewei Lu[1]
Key Laboratory of Bionic Engineering, Ministry of Education,
Jilin University,
Changchun 130025, China
e-mail: xwlu@jlu.edu.cn

Jianqiao Jin
Key Laboratory of Bionic Engineering, Ministry of Education,
Jilin University,
Changchun 130025, China
e-mail: jinjq19@mails.jlu.edu.cn

Lei Ren[1]
Key Laboratory of Bionic Engineering, Ministry of Education,
Jilin University,
Changchun 130025, China
e-mail: lren@jlu.edu.cn

Wei Liang
Key Laboratory of Bionic Engineering, Ministry of Education,
Jilin University,
Changchun 130025, China;
China Railway Construction Heavy Industry Co., Ltd.
Changsha 410100, China
e-mail: weiliang@jlu.edu.cn

Luquan Ren
Key Laboratory of Bionic Engineering, Ministry of Education,
Jilin University,
Changchun 130025, China
e-mail: lqren@jlu.edu.cn

ABSTRACT

Limb loss affects many people from a variety of backgrounds around the world. The most advanced commercially available prostheses for transfemoral amputees are fully active (powered) designs but remain very expensive and unavailable in the developing world. Consequently, improvements of low-cost, passive prostheses have been made to provide high quality rehabilitation to amputees of any background. This study

[1] Corresponding author.

explores the design and evaluation of a smooth-locking-based bionic knee joint to replicate the swing phase of the human gait cycle. The two-part design was based on the condyle geometry of the interface between the femur and tibia obtained from MR images of the human subject, while springs were used to replace the anterior and posterior cruciate ligaments. A flexible four-bar linkage mechanism was successfully achieved to provide not only rotation along a variable instantaneous axis but also slight translation in the sagittal plane, similar to the anatomical knee. We systematically evaluated the effects of different spring configurations in terms of stiffness, position and relaxion length on knee flexion angles during walking. A good replication of the swing phase was achieved by relatively high stiffness and increased relaxation length of springs. The stance phase of the gait cycle was improved compared to some models but remained relatively flat, where further verification should be conducted. In addition, 3D printing technique provides a convenient design and manufacturing process, making the prosthesis customizable for different individuals based on subject-specific modelling of the amputee's knee.

INTRODUCTION

Lower limb amputations were mainly classified as toe, foot and/or ankle, transtibial (below knee), and transfemoral (above knee). In the United States alone, there were 266,465 such operations from 1988 to 1996 [1]. There are several factors contributing to this number, with the rise in diabetes being one of the leading causes of the lower limb amputation worldwide. Diabetes causes neuropathy and circulation problems in the lower extremities which leads to foot ulceration, usually followed by a toe, foot/ankle, or transtibial amputation [2-4]. They have the potential to further develop into a transfemoral amputation with a 26% chance of a secondary amputation within the first 12 months of the initial amputation [5]. Another cause for the increased number of amputees comes with the improvement of body armor which has seen a decrease in the lethality of war wounds. More soldiers are returning from war with blast injuries to the extremities which require amputation [6]. As a result, there are many people in the west living with transfemoral limb loss, and the solution is to apply a prosthetic to the remaining limb which is used to mimic the look and function of a human leg.

Transfemoral amputees suffer from slower walking speeds, cosmetic issues and consequently a more limited, less fulfilled quality of life. There are a wide range of transfemoral prostheses available attempting to mitigate these problems. Prostheses can be divided into three major categories: passive (not powered), semi-active (partially powered) and fully active (powered) [7-9].

Fully active models are being developed to provide an optimized, realistic gait pattern [10-12]. Complex control methods are being proposed to interpret signals from the brain and other sensors to allow intuitive control of the prosthesis [13-15]. Sensory schemes (such as Echo Control and Gait-Mode Recognition [7], Electromyography [16, 17], Wearable Sensory Apparatus [13], Electroencephalography [18], Mechanomyography [18], etc.) are used to provide information on the user's current gait, the terrain or even neurological signals to a control system which trigger actuators accordingly. Such advanced technologies have been implemented into commercial devices as Power knee [19] and Linx [20]. However, high price and energy consumption are the main shortcomings.

Semi-active, microprocessor-controlled prostheses use variable damping systems such as pneumatic or hydraulic cylinders to provide swing phase control of the knee joint [21-24]. In pneumatic prostheses, the damping in the swing phase varies based on altering the size of the valve through which air can travel. This is adjusted before use according to the user's preference. However, if a microprocessor is adopted, sensors in the prosthesis can detect real time changes in swing speed and adjust the opening accordingly. Johansson *et al*. [25] conducted a comparative study on three prostheses (two microprocessor-controlled knees, the Rheo and C-Leg, along with the passive Mauch SNS) to determine the advantage of microprocessors and variable damping mechanisms over mechanically passive designs. It was found that the Rheo and C-Leg offered significant advantages over the mechanically passive Mauch SNS, which included a reduction in work done by the hip, improved stance stability and an increased smoothness of gait. The results suggested that a magnetorheological fluid was preferred, the metabolic rate was found to decrease when compared to the other two mechanisms [25]. These prostheses are highly effective, which allow for more complex ambulation such as ascending a staircase/ramp and variations in walking speed. However, they are expensive and inaccessible to those from poorer backgrounds.

While advanced technologies such as sEMG and sensory controls are being developed, passive low-cost designs are still being improved with the aim to build upon the very basic cheaper models available. The most rudimentary of which use a single axis hinge and locking mechanism to allow for limited ambulation [26, 27], such as the Committee of the Red Cross (ICRC) manual-locking knee [28] and the LCKnee automatic-locking knee [29]. Then, the polycentric mechanisms [30] provide further improvement to the basic hinge model, such as JaipurKnee, ReMotion Knee [31] and LeTorneau Polycentric Knee [32]. The typical design uses four points of rotation to allow for improved early stance stability [26]. The above designs are used primarily in the developing world due to their low cost but provide a more restricted gait than advanced semi-active and active designs. However, these designs offer little to accurate swing phase control [26], which is important for a natural and variable gait.

New innovative passive models are being developed to increase accessibility to high quality prostheses. An innovative concept design [33, 34] using the polycentric principle was developed based on the geometry of the femoral condyles and internal springs providing the function of the ACL and PCL ligaments. This biomimetic, passive design was 3D printed and provided positive results. However, it was not complete in mimicking the knee flexion angle for the gait cycle and had not studied the influence of the spring ligaments. Another impressive model [35] used a combination of tuned springs and dampers to engage and disengage as the hip moment of the amputee changed. This design is an exciting alternative to many passive designs currently available. The early stance peak flexion is difficult to replicate with passive prostheses because, to improve stability and avoid buckling, a stiff peg-leg like gait is often adopted in stance. It is difficult to achieve this change in flexion without active systems. Nevertheless, the clever design provides a potential unpowered solution to this which could be adopted by future designs. However, in terms of biomimicry, the physical design doesn't closely represent the human knee, and the profiles of the prosthetic knee are fixed which could not adjust for different individuals.

The function of a prosthetic leg can be greatly improved by the damping mechanism in the knee, along with the joint design. A knee utilizing optimized swing phase control in parallel with a polycentric knee will achieve a much-improved gait and stability when compared to more basic models. Using these two technologies will also allow for the amputee to move at a range of self-selected walking speeds.

This paper designs and evaluates a smooth-locking-based customizable transfemoral passive prosthetic knee joint, aiming to replicate the swing phase of the human gait cycle and to provide a relatively natural experience for the user. Inspiration was taken from nature by first analyzing the anatomy and function of the human knee, in accordance with the bionic principles. The design centered around a 3D-printed, two-part mechanism inspired from the human knee joint structures in conjunction with springs replacing the functions of the ACL and PCL ligaments. A flexible four-bar linkage mechanism based on an RPR chain was then obtained to allow the prosthetic knee be able to rotate along a variable instantaneous axis and slightly translate in the sagittal plane, similar to the anatomical knee. Gait experiments of different spring configurations in terms of stiffness, position and relaxation length have been conducted. The knee flexion angle during gait will be used as the primary indicator to evaluate each of the design. By exploring the use of 3D printing, this prosthetic knee joint is accessible for customization based on each individual’s dimensions.

METHODS

Inspiration and Principles

To design a functional transfemoral prosthesis, it is important to appreciate and understand the biology and biomechanics of the leg system. The knee joint system comprises of the femoral and tibial condyles, the patellofemoral joint, the menisci and the cruciate and collateral ligaments [36-39]. The resulting motion of the knee joint during flexion and extension is complex and cannot be accurately imitated by a simple hinge. The knee joint is best described mathematically as a polycentric joint. During flexion and extension, the femoral and tibial condyles roll and slide over one another to achieve a complex motion of the knee in which the center of rotation is constantly changing.

A biomimetic approach (**Figure 1**) is being used, which assumes that the closer the design replicates the anatomical knee joint, the better an approximation it should be. The shapes of the femoral and tibial condyles in the sagittal plane were replicated and incorporated into a polycentric hinge. The function of the anterior and posterior cruciate ligaments were replicated by springs which were widely used in many mathematical models of the knee joint [40-42]. The human knee joint in the sagittal plane [43] is shown in **Figure 1(a)**. The significant feature to consider is the crossed positioning of the cruciate ligaments in relation to the condyle interface of the distal femur.

Initial sketches for the biomimetic design were shown in **Figure 1(b)**. The upper section represents the distal femur, and the lower section represents the proximal tibia. The posterior of each section is curved to replicate the condyle interface, based on reconstruction of the human knee joint. As shown in **Figure 1(c)**, the geometry was achieved by taking an average of MR image data from the human subject in a resolution of 192 × 192 pixels, with each pixel containing 24 bits of gray tone. The upper section also has an extruded front which is used to ‘lock’ the knee joint at full extension. For the final design, two semi-circular gears in an approximate 1:1 gear ratio (**Figure 2**) were added to the flat interface between the upper and lower sections to help guide the lower section into the locking position, while minimizing the restriction to motion. The two sections are connected by a four-bar linkage system whose kinematic chain is an RPR chain. This system provides the function of the medial and lateral collateral ligaments along with the function of the ACL and PCL (green and red respectively) which vary in length during flexion and extension.

Ligament spring calculations

The ACL and PCL springs are the most significant parts to tune the position and shape of the four-bar linkage mechanism as they contribute to the response of the prosthesis during flexion and extension. Tension springs will be mounted on aluminum pins with notches to keep the springs in place (**Figure 2**). **Figure 3(a)** shows the generalized construction of the linkage and the extensions of the springs with increasing flexion, where $\boldsymbol{r_i}$ is the link vector and θ_i is the angle between $\boldsymbol{r_i}$ and the horizontal line (counter clockwise is positive). In this study, $\boldsymbol{r_2}$ and $\boldsymbol{r_3}$ represent the ACL and PCL, respectively. There are two assumptions made in this model: one is that the length r_6 remains constant; another is that the flexion angle, 2θ is double the angle that the length r_6 makes with the vertical axis, θ, which is an approximation due to the characteristics of the two gears. These assumptions were only proposed because they were convenient to simplify the analysis. The length of r_2 and r_3 along with θ_1 and θ_2 could be calculated as follows:

$$\begin{cases} r_1\cos(\theta_1)+r_2\cos(\theta_2)=r_3\cos(\theta_3)+r_4\cos(\theta_4) \\ r_1\sin(\theta_1)+r_2\sin(\theta_2)=r_3\sin(\theta_3)+r_4\sin(\theta_4) \\ r_5\cos(\theta_5)+r_6\cos(\theta_6)+r_7\cos(\theta_7)=r_3\cos(\theta_3) \\ r_5\sin(\theta_5)+r_6\sin(\theta_6)+r_7\sin(\theta_7)=r_3\sin(\theta_3) \end{cases} \tag{1}$$

The lengths were chosen by drawing the four-bar linkage onto the sagittal plane and scaling appropriately based on the size of the femur (**Table 1)**. Length r_7 and r_8 were kept constant for symmetry. The external link length, r_6 was fixed due to the geometry of the condyles. The length of r_5 was changed to determine the impact of increasing the tension in the PCL (r_3), and the two lengths were 15 mm or 30 mm, respectively. Finally, r_4 was set between these two values (r_5 and r_6). Using two values for the upper link length, r_5 allows for a comparison of the different polycentric knees. The shorter length could provide the prosthesis with a posterior 'elevated center', offering more stability for slow or older walkers. A longer length will increase the initial extension and moment induced, which could make the knee joint more responsive to small changes in hip moment.

Spring moments

The prosthesis knee is driven by the hip moment along with the ligament springs. A range of springs with varying constants (**Table 2**) are used to optimize the design. The moment induced by the springs can be calculated using the extension and angle of each spring. The forces exerted on the lower section of the knee joint are shown in **Figure 3(b)**. For all calculations d_2 ($r_4 - r_7$) is 25 mm and d_3 (r_7) is 15 mm, explained in the four-bar vector diagram above. Assuming clockwise is positive and rotation about the center point between d_2 and d_3, the resultant moment of the two springs M_{springs} is:

$$M_{\text{springs}} = d_3 k_{\text{PCL}} x_3 \sin(\theta_3) - d_2 k_{\text{ACL}} x_2 \sin(\theta_2) \quad (2)$$

where k_{ACL} and k_{PCL} are the stiffness of the ACL and PCL spring respectively, x_2 and x_3 are the elongation of the ACL and PCL spring respectively.

The springs had stiffness ranging from 200 – 1000 N/m as well as relaxation lengths from 45 mm – 60 mm. Using MATLAB (MathWorks, USA), a short program was used to investigate the relaxation length versus spring constant k to predict the moment generated (**Figures 4**). They were used in conjunction with trial and error to tune the knee parameters, such as flexion angles and moments [44]. The springs available are highlighted on the contour plots by dark triangles (**Figure 4**), three of which were chosen: a ‘weak’ spring of 203 N/m, a ’strong’ spring of 981 N/m and a ‘medium’ stiffness spring of 466 N/m. They were used as variables to investigate the effect of different spring configurations on knee flexion during walking, especially in swing phase.

The springs were chosen based on length and constant which could achieve a prosthetic knee joint moment vs angle curve that is similar to an anatomical swing phase. Based on the free body diagram of the thigh and eliminating the inertia angular moment of thigh, the springs induced knee moment M_{knee} could be calculated as below,

$$M_{\text{knee}} + M_{\text{hip}} - M_{\text{spring}} = 0 \tag{3}$$

where M_{hip} is the moment of the hip from the literature [44], and M_{springs} is the moment induced by the springs on the lower section. **Figure 5** shows the prosthetic knee moment using an ACL of 203 N/m and a PCL of 981 N/m compared to the actual moment of the knee during walking. Human knee moment data was derived from the literature [44]. Clearly, the swing phase of the gait cycle is best matched by this spring configuration.

Prototype and Manufacture

Figure 2 shows the final design of the smooth-locking-based prosthetic knee joint. The two curved gear sections inserted with several cylindrical pins are obtained according to the condyle geometry, and the central section contains the ligament springs mounted on pins. Each end of the spring is considered as a hinge joint with one degree of freedom (DoF). The multiple spring placements were used to change the ligament spring positions. External links were used to connect the two gear sections by bolts and to provide support for the prosthetic knee during walking. Each end of the link contained one rotating DoF. A slot extending downward with one translational DoF was added to the external links, which allowed the lower section to 'unlock' and extend away from the upper section during the swing phase. These features composed a flexible four-bar linkage mechanism, which could not only rotate along a variable instantaneous axis but also slightly translate in the sagittal plane, similar to the anatomical knee. Two semi-circular gears were used to provide a means for relocation when the knee is locked in the stance phase, and more gentle transition from stance to swing phase during walking.

A 3D printer (S5, Ultimaker B.V., The Netherlands) was used to manufacture the prototype. The Dark PLA material with 40% infill was used for 3D printing the knee joint structure. The lighter material is a soluble support structure. The design weighs approximately 300 g.

Data collection

Due to limitations in resources, the experiments were conducted on an able-bodied participant (male; age 26; mass 76.32 kg; height 1.76 m), same as the subject involved in obtaining the MR image. A hands-free crutch (iWALK 2.0, iWALKFree, Canada) used by patients suffering below knee injuries was redesigned. The final prosthetic design has two cylindrical extrusions which slide into the crutch to be securely fixed with bolts.

The crutch allows for an able-bodied subject to walk with the prosthetic knee in place of their own, just below their anatomical knee.

This study was conducted in accordance with the principles embodied in the Declaration of Helsinki and in accordance with local statutory requirements. All participants were provided written informed consent in accordance with the policies of the ethics committee of Jilin University. They were asked to walk on an 8 m long walkway with self-selected speed. Knee flexion angles were collected at 200 Hz using a six-infrared camera motion capture system (Vicon, UK). A high-speed camera (Phantom v1612, Vision Research Inc., USA) was mounted at a height of 0.58 m (this height was defined through trial and error) to record the motion with a resolution of 1280 × 800 pixels at 240 FPS. The camera was positioned perpendicularly from the center of the walking path. Under each condition of the different spring configurations, the representative walking data were ensured by repeating 15 times of the gait measurement.

Data processing

To compare the feature between the able-bodied walking and the prosthesis knee walking, eight identifiable stages during the stance and swing phases of the gait cycle were defined [45]: initial contact, contralateral toe off, heel rise, initial contact of the contralateral limb, toe off, swing limb, vertical tibia, and next initial contact (**Supplementary Figure S1, top**). The video files were edited in the software to produce the gait cycle diagrams. They were carefully identified and chosen frame by frame until reaching one of these eight stages (**Supplementary Figure S1, bottom)**.

Each spring configuration will be compared with the normal walking gait. The statistical analysis was performed to evaluate how the average of maximum knee flexion angle during swing phase change with different spring configurations using SPSS 20.0 software (IBM, United States). For each condition, means and standard deviations were calculated across all trials. They were then analyzed separately by using the analysis of variance (ANOVA) with repeated measurements based on a linear mixed model (random effects: trials; fixed effects: spring configurations; $p < 0.05$).

RESULTS

Altering ACL/PCL spring stiffness

The first set of experiments was to investigate the effects of varying the ACL and PCL spring stiffness on knee flexion during the gait cycle. Longer PCL configuration were used (**Figure 6**). Five spring combinations with same relaxion length of 46 mm were tested using a range of spring strengths: weak, medium and strong (Spring 1, 2 and 4), along with no-spring configuration. The knee flexion angle of each configuration (**Figure 6**) were measured and the posture of the eight key stages during gait cycle (**Supplementary Figure S2**) were observed. **Table 3** shows the gait characteristics for different combinations of the ACL and PCL spring stiffnesses.

Compare with able-bodied walking, there is no significant change for the no-spring prosthetic knee during the stance phase. However, a sudden leap in flexion angle occurs at around 55% gait, which is clearly induced from the start of the swing phase. The knee then reaches a maximum flexion angle and then decreases toward the heel strike (terminal swing). The distinctive table-top shape of the knee flexion curve was observed as no spring forces were provided during swing.

The configuration of Weak ACL – Medium PCL clearly improves the response. The prosthesis reaches the maximum flexion more gradually, although a significantly lower flexion angle than the able-bodied ambulation. But, this configuration peaks too early and falls away rapidly during mid swing, indicating a rapid swing back mechanism to the locking position. A stronger PCL was then adopted as the anatomical knee suggested, but proved too strong for design, causing the knee joint to excessively bend during stance until buckling (**Supplementary Figure S2**). Multiple trials were tried to complete the gait cycle, even with very slow walk and with little weight on the prosthesis, but no successful walking was obtained.

The configuration of Weak PCL – Medium ACL (opposite to the anatomical knee) shows a similar response to the no-spring configuration, but the time-angle curve is damped. The knee remains at a constant angle for the entire stance phase before rapidly increasing from pre-swing to mid-swing. The flexion angle increases slightly before dropping off during late-swing. **Supplementary Figure S2** shows that the contralateral leg was working hard to provide momentum to the prosthesis. Stronger ACL ligament was then substituted to see if the damping effects would be exacerbated. Contrarily, the knee flexion shows an improved peak angle under Weak PCL – Strong ACL. A higher peak flexion is achieved and reached at a steeper gradient, more like the able-bodied knee. The same snap-back of the knee during late to terminal-swing is still evident by a rapid decrease in flexion angle at around 90% gait.

To highlight the geometry of the four-bar spring layout, two identical, medium strength springs (Medium ACL – Medium PCL) were used. The very low peak flexion angle indicates that to some degree, using springs of a similar strength will balance each other out rather than assist the swing of the shank. This is observed in **Supplementary Figure S2** which shows that the foot of the prosthesis remains very close to the ground.

Altering PCL Spring Position

The configuration of Weak ACL – Strong PCL and Weak PCL – Strong ACL (one strong and one weaker ligament) were repeated with a shorter PCL configuration (**Figure 7**). As discussed above, the moment arm was too large for the strong PCL using the long PCL configuration (Weak ACL – Strong PCL), which caused the knee to buckle. This is improved by setting Strong Short PCL, which demonstrates a smoother gait as shown in **Figure 7(c)**. This may be due to the decreased moment arm and extensions involved. The overall shape of this knee flexion is promising.

The two results of changing PCL position under the configuration of Weak PCL – Strong ACL are more comparable. The short PCL provides the best stance phase of all previous tests, even displaying a small and delayed peak compared to the able-bodied. The terminal stance transition into swing is closer to the able-bodied. The transition from late to terminal swing is different to the other configurations, decreasing more gradually towards terminal swing as shown in **Figure 7(b)**. The peak of knee flexion is offset either side of the able-bodied for both the short and long PCL.

Altering Relaxation Length

The effect of spring relaxation length on the knee flexion angle has been studied in this section. The configuration of Weak ACL – Strong Short PCL and Strong ACL – Weak Short PCL were repeated by changing the strong (981 N/m) spring with long relaxion length of 56 mm (Spring 5), 10 mm longer than the original one (**Figure 8**). Under Weak ACL – Strong Short PCL, the longer relaxation length appears to have a more human-like swing phase, reaching a high peak flexion at around 70% gait cycle similar to the able-bodied. This may be caused from the fact that the longer relaxation length of PCL could induce a decreased moment during extension compared to the shorter one. The gait cycle in **Figure 8(c)** shows this smoother gait, especially for the contralateral foot which appears unstretched.

For the configuration of Strong ACL – Weak Short PCL, the two different spring lengths have similar trends. The overall shape of the swing phase with longer relaxation length is improved, increasing and decreasing at a similar gradient to the able-bodied. The swing phase is the best reproduction of the normal ambulation in all the configurations. However, the stance phase is limited, reducing in flexion during pre-swing rather than continuing to increase. Despite this, the overall gait cycle shows a very smooth trend with each phase of walking replicated well by the prosthetic knee.

DISCUSSIONS

Optimal Design Kinematics

The two curved gear sections, adjustable ligament springs, and external links with sliding slot composed a flexible four-bar linkage mechanism of the prosthetic knee in this study. Similar to human knee, it could not only rotate along a variable instantaneous axis but also slightly translate in the sagittal plane. With proper spring configurations in terms of stiffness, position and relaxion length, the prosthetic knee could achieve similar knee flexion angles during walking gait with those of able-bodied knee. The best results obtained from the experiments are clearly those using the long relaxation length springs.

When comparing to the able-bodied gait, the stance phase of some tests appears to be the least accurate, showing little variation before dipping at toe off. This is likely due to the gears locking in the transition from stance to swing, especially with no springs. It was improved upon in several configurations such as the short PCL (**Supplementary Figure S2**). The strong ACL combining with a slightly raised center of rotation, posterior to the knee joint, improves the stance stability and suggests that the knee will not flex unless a significant moment of the hip is exerted. Accordingly, the subject feels more confident in the walking gait and can flex the knee slightly in stance phase, knowing that the prosthesis will not buckle due to the raised center. However, this may inhibit the flexion during swing leading to a low maximum flexion angle.

Generally, the different configurations have allowed for improved transition from stance to swing. Many of the configurations above show a drastic initial rise in knee flexion at toe off before the springs begin to take control of the motion as shown in **Figure 8(a)**. Mitigating this jump was achieved in **Figure 8(b)** with a much gradual transition into mid swing. During swing phase, many configurations are clearly slight transformations of the ‘table-top’ diagram for the no-spring configuration (**Figure 6, light grey**), in which the transition from stance to swing shows a large jump as the knee joint fully unlocks. After the initial jump, the springs extending enough begin to induce an adequate moment to either balance out the swing or further increase the flexion angle. **Figure 8(a)** shows how this table-top was controlled by the springs when compared to no springs.

The gait pattern of the swing phase varied as it was influenced mainly by the spring configuration. The first notable concern is that the average peak flexion is not very high for any of the experiments, with the highest no more than 50 degrees (**Figure 6**). This low peak value may be caused from the excessive friction in the prosthetic knee joint. The most human-like swing phase was found for the long PCL relaxation length as shown in **Figure 8(a)**, displaying the gradual increase to peak flexion and decrease with terminal swing to heel strike.

Commercial Product Comparison

For the transfemoral amputees, great efforts have been made on developing the prosthetic knees that aims to reproduce the natural gait during daily tasks, especially for walking. Segal *et al.* [46] conducted a kinematic and kinetic analysis of two advanced prostheses, the microprocessor-controlled C-Leg and the Mauch SNS. Both of which use complex variable damping technologies. The variable damping knees have very similar curves to the able-bodied gait, with a flat stance phase followed by a large peak during the swing phase. The only major difference was the slightly higher peak flexion shown by the Mauch SNS. Even though this study was conducted in 2006, the same technologies are used today [47].

Comparing these commercial models to the smooth-locking-based prosthetic knee joint, given the differences in resources, a good approximation of the gait cycle was achieved. The stance phase is relatively constant and the swing phase in-line with the able-bodied knee. We compare the design principles and the functional parameters with the existing prostheses (Table 4). It can be seen that the proposed bionic knee can provide comparable swing-phase joint motion angle and moment to those of some advanced prostheses (semi-active or passive) at low cost and low weight, meanwhile it can also be personalized for different individuals according to the derived medical images of bones and ligaments. This implies that with some further tuning, the proposed smooth-locking design could be a viable low-cost alternative for transfemoral amputees.

Limitations and future work

The most significant limitation of this design is the inconsistent swing phase. The peak flexion angle rarely occurs in the correct region (60% – 80% gait) and is also not high enough in magnitude. However, tuning of the knee joint does give some promising results (**Figure 8**). Although some minor improvements have been made in the stance to swing transition, the smooth transition was not always evident. Also, the in-stance flexion at 15% – 20% gait cycle shown in the able-bodied walking **(Figure 6**) is completely absent as, when in the stance phase, the knee joint is locked into a straight position only allowing for very small flexion before the swing phase. These may be caused from the fact that the anterior and posterior cruciate ligaments in humans are highly nonlinear, but they are simplified as linear springs in this study. Potential solutions to achieve this property while still providing stability should be investigated. A multiple damping/clutch system similar to that used by Arelekatti and Winter [35] could be a starting point to provide more realistic mechanical characteristics. Besides, a prosthetic foot should be included in the future as it plays an important role in the gait.

Besides, the knee flexion angle was obtained based on an open source video motion analysis software. Ideally, 3D motion tracking technology would be a preferable alternative for more accurate results. Also, only healthy subject conducted the experiments. Gait speeds may affect the knee flexion angles and moments. However, it is quite inconvenient to naturally change walking speeds by the healthy subject wearing a prosthesis. In future, amputees should be involved not only in the gait measurements but also in the beginning of the design process. The MR images should be captured from the specific amputee and the condyle geometry of the prosthesis be customized for individuals. We mainly measured the knee flexion angles but not included the moments of the prosthetic knee. Ground reaction forces and moments should be considered when calculating the moments of prosthetic knee, which are not able to be measured in this study. We will conduct more experiments with the force plate instruments in the future to investigate the knee moments generated with the prosthetic knee.

ACL and PCL springs are the most significant parts to tune the position and shape, so the adjustment of the two springs is critical. However, the adjustment in this paper is carried out mostly by manual operation. In future, some adjustment mechanisms can be incorporated in the prototype. Also, the mechanical properties of the prosthetic knee need further testing, a rig could be designed to test the prosthesis for a predetermined distance for wear and fatigue failure. Alternative parts such as bearings to increase the peak flexion angle during swing should be explored, as it is hypothesised that frictional losses are the reason for the low peak flexion angle. Metal 3D printed materials such as aluminium alloy or stainless steel should be also considered to improve the practicality.

CONCLUSION

Low cost, passive prostheses are being developed to increase the access to high quality prosthetic knee joints. This paper proposed an alternative smooth-locking-based passive prosthesis inspired from the geometry and biomechanics of human knee joint. A flexible four-bar linkage mechanism was successfully achieved from the integration of two curved gear sections, adjustable ligament springs, and external links with sliding slot. This mechanism provided not only rotation along a variable instantaneous axis but also slight translation in the sagittal plane, similar to the anatomical human knee. With proper spring configurations in terms of stiffness, position and relaxion length, the prosthetic knee could achieve similar knee flexion angles with those of able-bodied knee especially during swing phase. As expected, the swing phase was heavily varied and largely controlled by the range of spring configurations tested. It was found that using springs with relatively high stiffness, but an increased relaxation length gave the smoothest results, as shorter springs induce a greater moment for the same extension and stiffness which overpowered and skewed the angles of the knee during swing. The proposed bionic prosthetic knee performs well when compared with commercial prostheses, which indicates that access to more human resources and further testing of the design would provide a commercial product for the transfemoral amputees. The design is relatively low cost and has the potential to be extremely customizable for different individuals. Highly personalized design and manufacturing of the prosthetic knee, based on the subject-specific modelling of the anatomical human knee, could be adjusted for different amputees. In future, continuing the bionic approach by embracing the use of variable dampers and clutches would potentially lead to increased costs with actuators used to replicate more muscle and ligament function.

FUNDING

This research was partly supported by the National Key R&D Program of China under No. 2018YFC2001300, the National Natural Science Foundation of China under No. 52005209, No. 91948302, No. 91848204, No. 52021003, and the Natural Science Foundation of Jilin Province under No. 20210101053JC.

Conflict of Interest

There are no conflicts of interest.

REFERENCES

[1] Smith, D. G., 2004, "The Transfemoral Amputation Level, Part 1," inMotion, 14(2), pp. 54-58.

[2] Lavery, L. A., Ashry, H. R., van Houtum, W., Pugh, J. A., Harkless, L. B., and Basu, S., 1996, "Variation in the incidence and proportion of diabetes-related amputations in minorities," Diabetes Care, 19(1), pp. 48-52.

[3] Fosse, S., Hartemann-Heurtier, A., Jacqueminet, S., Ha Van, G., Grimaldi, A., and Fagot-Campagna, A., 2009, "Incidence and characteristics of lower limb amputations in people with diabetes," Diabetic Med., 26(4), pp. 391-396.

[4] Hoffstad, O., Mitra, N., Walsh, J., and Margolis, D. J., 2015, "Diabetes, Lower-Extremity Amputation, and Death," Diabetes Care, 38(10), pp. 1852-1857.

[5] Kaufman, K. R., Levine, J. A., Brey, R. H., McCrady, S. K., Padgett, D. J., and Joyner, M. J., 2008, "Energy expenditure and activity amputees using mechanical and of transfemoral microprocessor-controlled prosthetic knees," Arch. Phys. Med. Rehab., 89(7), pp. 1380-1385.

[6] Gawande, A., 2004, "Casualties of war -- Military care for the wounded from Iraq and Afghanistan," New Engl. J. Med., 351(24), pp. 2471-2475.

[7] Windrich, M., Grimmer, M., Christ, O., Rinderknecht, S., and Beckerle, P., 2016, "Active lower limb prosthetics: a systematic review of design issues and solutions," Biomed. Eng. Online, 15, pp. 5-19.

[8] Gholizadeh, H., Abu Osman, N. A., Eshraghi, A., and Ali, S., 2014, "Transfemoral Prosthesis Suspension Systems A Systematic Review of the Literature," Am. J. Phys. Med. Rehab., 93(9), pp. 809-823.

[9] Price, M. A., Beckerle, P., and Sup, F. C., 2019, "Design Optimization in Lower Limb Prostheses: A Review," IEEE T. Neur. Sys. Reh., 27(8), pp. 1574-1588.

[10] Spanias, J. A., Perreault, E. J., and Hargrove, L. J., 2016, "Detection of and Compensation for EMG Disturbances for Powered Lower Limb Prosthesis Control," IEEE T. Neur. Sys. Reh., 24(2), pp. 226-234.

[11] Sup, F., Bohara, A., and Goldfarb, M., 2008, "Design and control of a powered transfemoral prosthesis," Int. J. Robot. Res., 27(2), pp. 263-273.

[12] Lenzi, T., Cempini, M., Hargrove, L., and Kuiken, T., 2018, "Design, development, and testing of a lightweight hybrid robotic knee prosthesis," Int. J. Robot. Res., 37(8), pp. 953-976.

[13] Parri, A., Martini, E., Geeroms, J., Flynn, L., Pasquini, G., Crea, S., Lova, R. M., Lefeber, D., Kamnik, R., Munih, M., and Vitiello, N., 2017, "Whole Body Awareness for Controlling a Robotic Transfemoral Prosthesis," Front. Neurorobotics, 11, p. 25.

[14] Obe, S. Z., Sykes, A., Lang, S., and Cullington, I., 2005, "Adaptive prosthesis - a new concept in prosthetic knee control," Robotica, 23, pp. 337-344.

[15] Heidarzadeh, S., Sharifi, M., Salarieh, H., and Alasty, A., 2019, "A Novel Robust Model Reference Adaptive Impedance Control Scheme for an Active Transtibial Prosthesis," Robotica, 37(9), pp. 1562-1581.

[16] Reaz, M. B. I., Hussain, M. S., and Mohd-Yasin, F., 2006, "Techniques of EMG signal analysis: detection, processing, classification and applications," Biol. Proced. Online, 8, pp. 11-35.

[17] Hefferman, G. M., Zhang, F., Nunnery, M. J., and Huang, H., 2015, "Integration of surface electromyographic sensors with the transfemoral amputee socket: A comparison of four differing configurations," Prosthet. Orthot. Int., 39(2), pp. 166-173.

[18] Song, S., and Geyer, H., 2015, "Regulating speed in a neuromuscular human running model," 2015 IEEE-RAS 15th International Conference on Humanoid Robots (Humanoids), IEEE, Seoul, Korea (South), pp. 217-222.

[19] Össur, "Power knee," https://www.ossur.com/en-us/prosthetics/knees/power-knee.

[20] Blatchford, "Linx," https://www.blatchfordus.com/products/linx.

[21] Sawers, A. B., and Hafner, B. J., 2013, "Outcomes associated with the use of microprocessor-controlled prosthetic knees among individuals with unilateral transfemoral limb loss: A systematic review," J. Rehabil. Res. Dev., 50(3), pp. 273-314.

[22] Kannenberg, A., Zacharias, B., and Probsting, E., 2014, "Benefits of microprocessor-controlled prosthetic knees to limited community ambulators: Systematic review," J. Rehabil. Res. Dev., 51(10), pp. 1469-1495.

[23] Fluit, R., Prinsen, E. C., Wang, S., and van der Kooij, H., 2020, "A Comparison of Control Strategies in Commercial and Research Knee Prostheses," IEEE T. Bio-Med. Eng., 67(1), pp. 277-290.

[24] Lee, J. T., Bartlett, H. L., and Goldfarb, M., 2020, "Design of a Semipowered Stance-Control Swing-Assist Transfemoral Prosthesis," IEEE-ASME T. Mech., 25(1), pp. 175-184.

[25] Johansson, J. L., Sherrill, D. M., Riley, P. O., Bonato, P., and Herr, H., 2005, "A clinical comparison of variable-damping and mechanically passive prosthetic knee devices," Am. J. Phys. Med. Rehab., 84(8), pp. 563-575.

[26] Tang, P. C. Y., Ravji, K., Key, J. J., Mahler, D. B., Blume, P. A., and Sumpio, B., 2008, "Let them walk! Current prosthesis options for leg and foot amputees," J. Am. Coll. Surgeons, 206(3), pp. 548-560.

[27] Andrysek, J., 2010, "Lower-limb prosthetic technologies in the developing world: A review of literature from 1994-2010," Prosthet. Orthot. Int., 34(4), pp. 378-398.

[28] Jensen, J. S., and Raab, W., 2004, "Clinical field testing of trans-femoral prosthetic technologies: resin-wood and ICRC-polypropylene," Prosthet. Orthot. Int., 28(2), pp. 141-151.

[29] Andrysek, J., Klejman, S., Torres-Moreno, R., Heim, W., Steinnagel, B., and Glasford, S., 2011, "Mobility function of a prosthetic knee joint with an automatic stance phase lock," Prosthet. Orthot. Int., 35(2), pp. 163-170.

[30] Mohanty, R. K., Mohanty, R. C., and Sabut, S. K., 2020, "A systematic review on design technology and application of polycentric prosthetic knee in amputee rehabilitation," Phys. Eng. Sci. Med., 43(3), pp. 781-798.

[31] Hamner, S. R., Narayan, V. G., and Donaldson, K. M., 2013, "Designing for Scale: Development of the ReMotion Knee for Global Emerging Markets," Ann. Biomed. Eng., 41(9), pp. 1851-1859.

[32] Ayers, S. R., and Gonzalez, R. V., 2010, "Implementation of a new polycentric knee technology in the developing world," Proceedings of the 13th World Congress of

the International Society for Prosthetics and Orthotics, ISPO, Leipzig, Germany, pp. 390-391.

[33] Ramakrishnan, T., Schlafly, M., and Reed, K. B., 2016, "Biomimetic transfemoral knee with a gear mesh locking mechanism," International Journal of Engineering Research and Innovation, 8(2), pp. 30-38.

[34] Ramakrishnan, T., Schlafly, M., and Reed, K. B., 2017, "Evaluation of 3D printed anatomically scalable transfemoral prosthetic knee," 2017 International Conference on Rehabilitation Robotics (ICORR), IEEE, London, UK, pp. 1160-1164.

[35] Arelekatti, V. N. M., and Winter, V. A. G., 2018, "Design and Preliminary Field Validation of a Fully Passive Prosthetic Knee Mechanism for Users With Transfemoral Amputation in India," J. Mech. Robot., 10(3), p. 031007.

[36] Goldblatt, J. P., and Richmond, J. C., 2003, "Anatomy and biomechanics of the knee," Oper. Techn. Sport. Med., 11(3), pp. 172-186.

[37] Bowman, K. F., and Sekiya, J. K., 2010, "Anatomy and Biomechanics of the Posterior Cruciate Ligament, Medial and Lateral Sides of the Knee," Sports Med. Arthrosc., 18(4), pp. 222-229.

[38] Choi, C. H., Kim, S. J., Chun, Y. M., Kim, S. H., Lee, S. K., Eom, N. K., and Jung, M., 2018, "Influence of knee flexion angle and transverse drill angle on creation of femoral tunnels in double-bundle anterior cruciate ligament reconstruction using the transportal technique: Three-dimensional computed tomography simulation analysis," Knee, 25(1), pp. 99-108.

[39] Piazza, S. J., and Cavanagh, P. R., 2000, "Measurement of the screw-home motion of the knee is sensitive to errors in axis alignment," J. Biomech., 33(8), pp. 1029-1034.

[40] Blankevoort, L., Kuiper, J. H., Huiskes, R., and Grootenboer, H. J., 1991, "Articular contact in a three-dimensional model of the knee," J. Biomech., 24(11), pp. 1019-1031.

[41] Beidokhti, H. N., Janssen, D., van de Groes, S., Hazrati, J., Van den Boogaard, T., and Verdonschot, N., 2017, "The influence of ligament modelling strategies on the predictive capability of finite element models of the human knee joint," J. Biomech., 65, pp. 1-11.

[42] Maloney, S. J., Richards, J., Nixon, D. G. D., Harvey, L. J., and Fletcher, I. M., 2017, "Do stiffness and asymmetries predict change of direction performance?," J. Sport. Sci., 35(6), pp. 547-556.

[43] Zavatsky, A. B., and O'Connor, J. J., 1992, "A Model of Human Knee Ligaments in the Sagittal Plane: Part 1: Response to Passive Flexion," P. I. Mech. Eng. H., 206(3), pp. 125-134.

[44] Lee, S. J., and Hidler, J., 2008, "Biomechanics of overground vs. treadmill walking in healthy individuals," J. Appl. Physiol., 104(3), pp. 747-755.

[45] Torricelli, D., Gonzalez, J., Weckx, M., Jimenez-Fabian, R., Vanderborght, B., Sartori, M., Dosen, S., Farina, D., Lefeber, D., and Pons, J. L., 2016, "Human-like compliant locomotion: state of the art of robotic implementations," Bioinspir. Biomim., 11(5), p. 051002.

[46] Segal, A. D., Orendurff, M. S., Mute, G. K., McDowell, M. L., Pecoraro, J. A., Shofer, J., and Czerniecki, J. M., 2006, "Kinematic and kinetic comparisons of transfemoral amputee gait using C-Leg (R) and Mauch SNS (R) prosthetic knees," J. Rehabil. Res. Dev., 43(7), pp. 857-869.

[47] Chien, M. S. C. H., Erdemir, A., van den Bogert, A. J., and Smith, W. A., 2014, "Development of dynamic models of the Mauch prosthetic knee for prospective gait simulation," J. Biomech., 47(12), pp. 3178-3184.

Figure Captions List

Fig. 1 Inspiration and design principles. (a) The human knee joint in the sagittal plane [43], left hand side-anterior, right hand side-posterior. (b) Design diagram showing ligaments at different states of flexion. (c) Reconstruction of the human knee joint.

Fig. 2 Final design of the smooth-locking-based prosthetic knee joint.

Fig. 3 Ligament spring calculations. (a) Four-bar vector diagram. (b) Moment induced by the springs on the lower section.

Fig. 4 Moment contour plot for the ACL and PCL spring with different constant and relaxation length. Available springs marked as triangles.

Fig. 5 Comparison between the springs induced prosthetic knee moment and the anatomical knee moment during swing phase. Human knee moment data was derived from the literature [44].

Fig. 6 Knee flexion angles using springs with different stiffness. Bars at right are the averages of the maximum knee flexion angle; n = 15; error bars, s.d.; p values indicate the results of ANOVA tests for an effect of spring configuration.

Fig. 7 Knee flexion angles (a), (b) and gait cycle diagrams (c), (d) using springs with different PCL position. Bars are the averages of the maximum knee flexion angle; n = 15; error bars, s.d.; p values indicate the results of ANOVA tests for an effect of spring configuration.

Fig. 8 Knee flexion angles (a), (b) and gait cycle diagrams (c), (d) using springs with different relaxion length. Bars are the averages of the maximum knee flexion angle; n = 15; error bars, s.d.; p values indicate the results of ANOVA tests for an effect of spring configuration.

Fig. S1 Eight identifiable stages during human walking.

Fig. S2 Gait cycle diagrams using springs with different stiffness.

Table Caption List

Table 1	Lengths and angles of four-bar vector components.
Table 2	Stiffness and relaxation lengths for all springs.
Table 3	Gait characteristics for different combinations of the ACL and PCL spring stiffnesses.
Table 4	Comparison with the existing prosthetic knees.

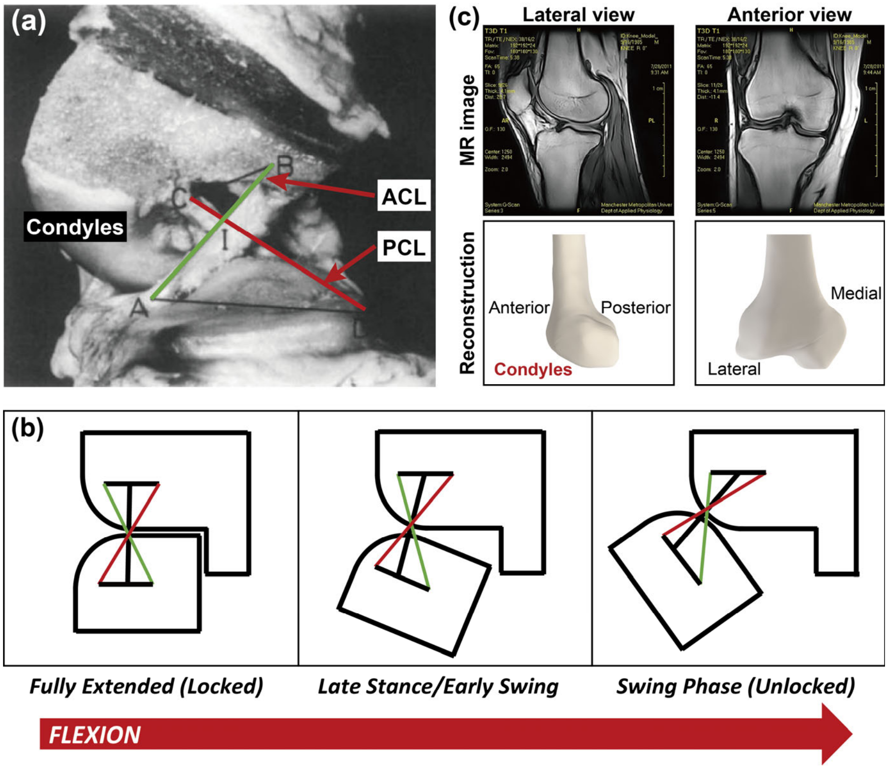

Figure 1. Inspiration and design principles. (a) The human knee joint in the sagittal plane [43], left hand side-anterior, right hand side-posterior. (b) Design diagram showing ligaments at different states of flexion. (c) Reconstruction of the human knee joint.

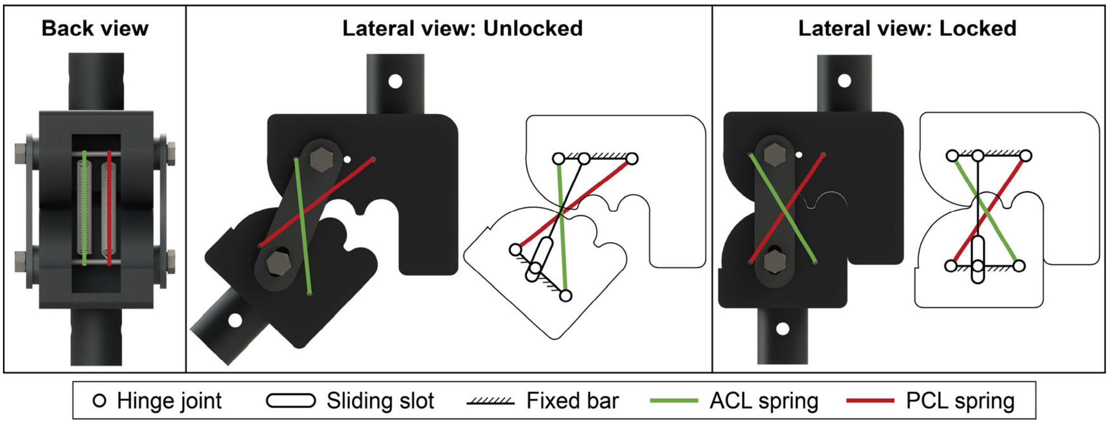

Figure 2. Final design of the smooth-locking-based prosthetic knee joint.

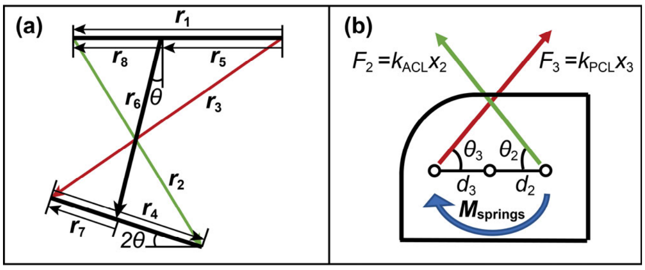

Figure 3. Ligament spring calculations. (a) Four-bar vector diagram. (b) Moment induced by the springs on the lower section.

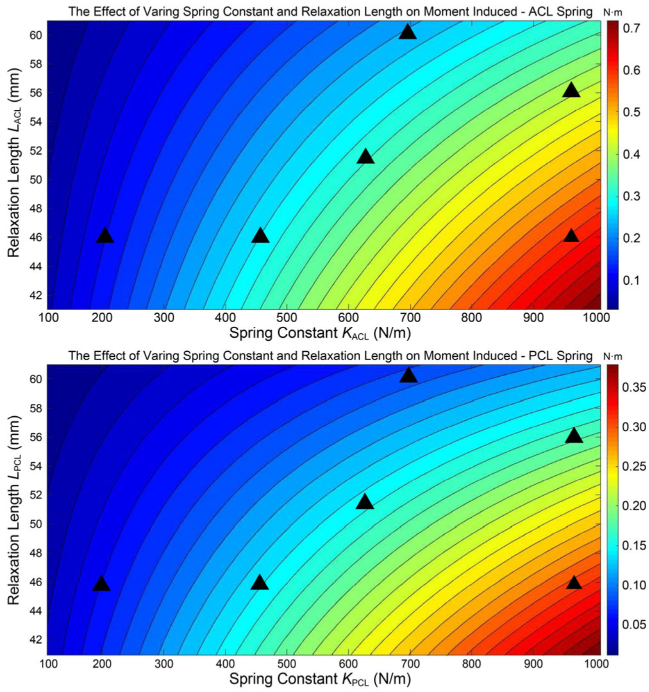

Figure 4. Moment contour plot for the ACL and PCL spring with different constant and relaxation length. Available springs marked as triangles.

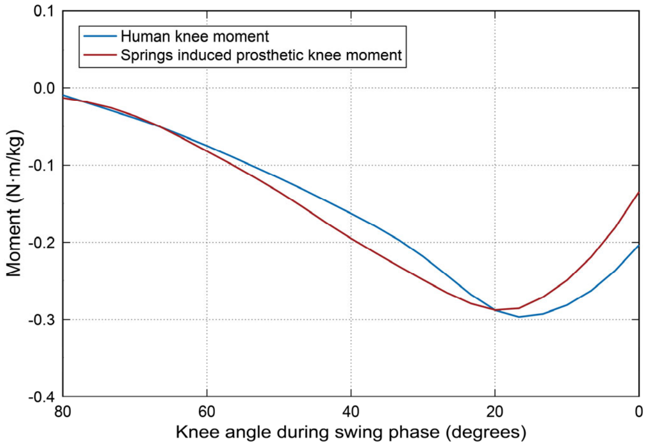

Figure 5. Comparison between the springs induced prosthetic knee moment and the anatomical knee moment during swing phase. Human knee moment data was derived from the literature [44].

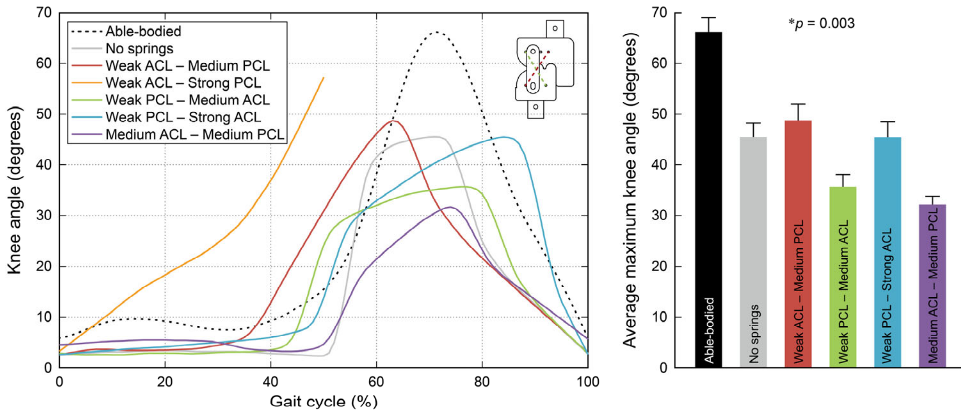

Figure 6. Knee flexion angles using springs with different stiffness. Bars at right are the averages of the maximum knee flexion angle; n = 15; error bars, s.d.; p values indicate the results of ANOVA tests for an effect of spring configuration.

691 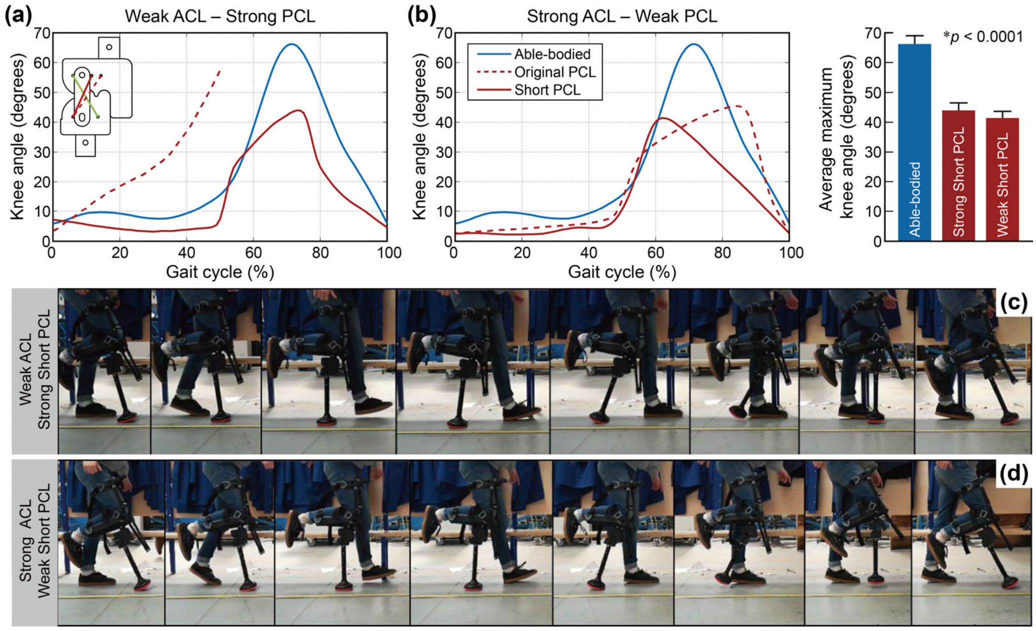

692 **Figure 7.** Knee flexion angles (a), (b) and gait cycle diagrams (c), (d) using springs with
693 different PCL position. Bars are the averages of the maximum knee flexion angle; *n* = 15;
694 error bars, s.d.; *p* values indicate the results of ANOVA tests for an effect of spring
695 configuration.

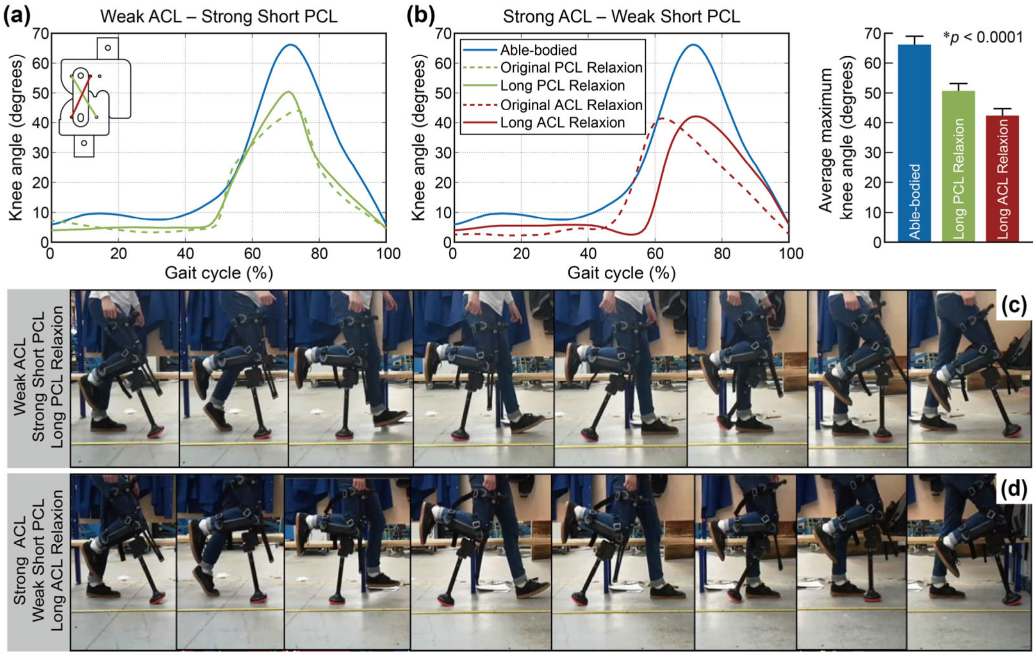

Figure 8. Knee flexion angles (a), (b) and gait cycle diagrams (c), (d) using springs with different relaxion length. Bars are the averages of the maximum knee flexion angle; n = 15; error bars, s.d.; p values indicate the results of ANOVA tests for an effect of spring configuration.

Table 1. Lengths and angles of four-bar vector components.

Length (mm)	**Angle (degrees)**
r_1 = 30 or 45	$\theta_1 = 0$
r_2 (ACL) = *Variable*	θ_2 = *Variable*
r_3 (PCL) = *Variable*	θ_3 = *Variable*
$r_4 = 40$	$\theta_4 = -2\theta$
r_5 = 15 or 30	$\theta_5 = 0$
$r_6 = 62$	$\theta_6 = 270 - \theta$
$r_7 = 15$	$\theta_7 = 180 - 2\theta$
$r_8 = 15$	$\theta_8 = 0$

Table 2. Stiffness and relaxation lengths for all springs.

Number	Relaxion Length (mm)	Stiffness (N/mm)
Spring 1	46	203
Spring 2	46	466
Spring 3	52	628
Spring 4	46	981
Spring 5	56	981
Spring 6	60	706

Table 3. Gait characteristics for different combinations of the ACL and PCL spring stiffnesses.

Combination	Peak joint angle (degrees)	Position of peak (% gait cycle)	RMSE (n = 101)	Relative RMSE (%)
Able-bodied	66.2	71	/	/
No springs	45.5	71	11.7	17.7
Weak ACL – Medium PCL	48.7	63	15.0	22.7
Weak ACL – Strong PCL	/	/	/	/
Weak PCL – Medium ACL	35.7	76	12.8	19.3
Weak PCL – Strong ACL	45.5	84	9.7	14.7
Medium ACL – Medium PCL	31.7	74	15.9	24.0

RMSE represents the root mean square error between the able-bodied and prosthetic knee.

Table 4. Comparison with the existing prosthetic knees.

Name	C-leg[46]	Mauch SNS[46]	LCKnee[29]	ReMotion[31]	This study
Mechanical design	Single-axis	Single-axis	Single-axis	Polycentric	Polycentric
Swing control	Microprocessor	Hydraulic	Spring	Spring	Ligament
Stance locking	Hydraulic	Hydraulic	Body weight + spring	Body weight + spring	Body weight + circular gear
Actuation	Semi-active	Passive	Passive	Passive	Passive
Weight (g)	1235	1140	/	618	415
Joint motion range (°)	130	115	120	160	180
Peak knee angle during swing (°)	55.2	64.4	/	32.2	50.1
Peak knee moment during swing (N·m/kg)	-0.24	-0.22	/	-0.23	-0.28
Customizable	no	no	no	yes	yes
Price (USD)	>40,000	>350	50 to 100	<80	30 to 50

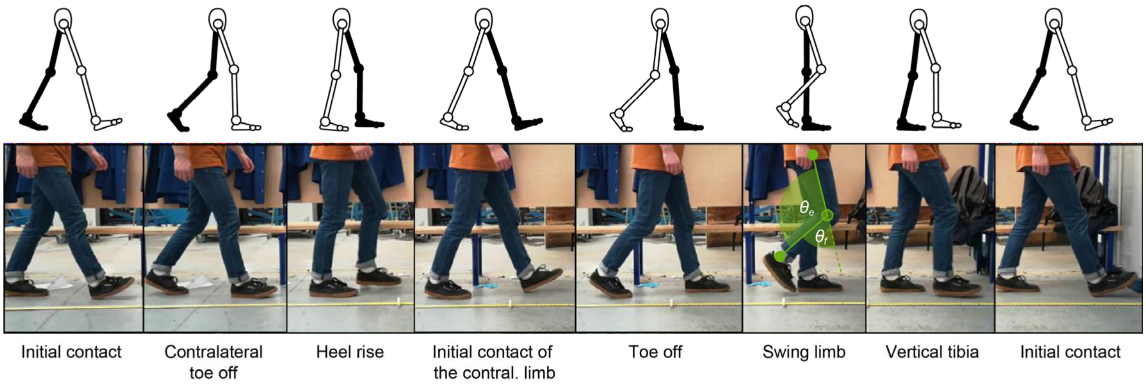

Supplementary Figure S1. Eight identifiable stages during human walking.

712 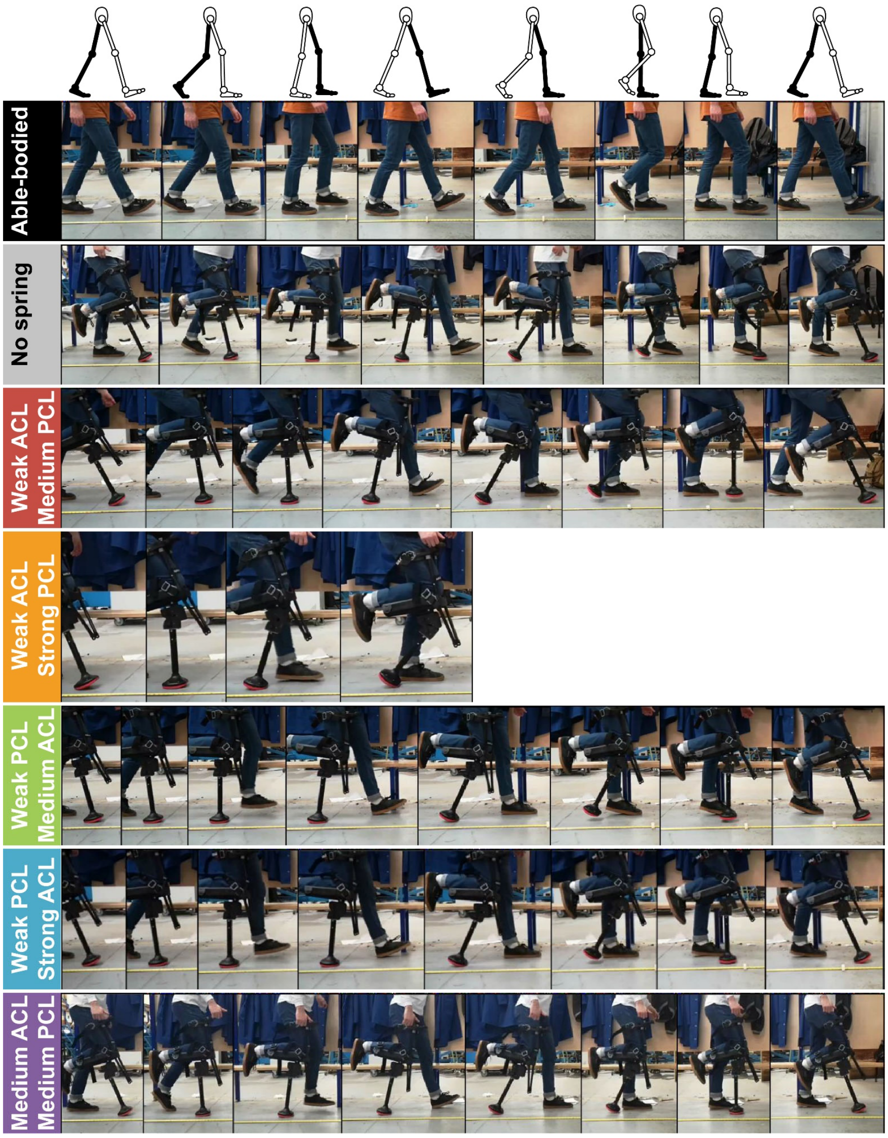

713 **Supplementary Figure S2.** Gait cycle diagrams using springs with different stiffness.

714